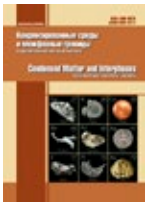

ISSN 1606-867X (Print)
ISSN 2687-0711 (Online)
Condensed Matter and Interphases
Kondensirovannye Sredy i Mezhfaznye Granitsy
https://journals.vsu.ru/kcmf/

Original articles

Research article
https://doi.org/10.17308/kcmf.2024.26/11941

Anodic dissolution and passivation of manganese monosilicide in fluoride-containing sulfuric acid solutions

I. S. Polkovnikov[1]✉, V. V. Panteleeva[1], A. B. Shein[1]

[1]Perm State University
15 ul. Bukireva, Perm 614990, Russian Federation

Abstract

The purpose of this study was to investigate the anode resistance of manganese monosilicide MnSi in fluoride-containing sulfuric acid solutions and the concentration effect of sodium fluoride on the anodic dissolution and passivation of the silicide.

The study was carried out on a single-crystal MnSi sample in 0.5 M H_2SO_4 + (0.0025–0.05) M NaF solutions. The study presents micrographs and elemental composition of the electrode surface after anodic polarization from *E* corrosion to *E* = 3.2 V in 0.5 M H_2SO_4 and 0.5 M H_2SO_4 + 0.05 M NaF solutions. A stronger etching of the electrode surface was observed in the presence of fluoride ions; elemental analysis showed an increase in the oxygen content in certain areas of the silicide surface associated with the formation of manganese and silicon oxides and their partial removal at high polarization values.

The kinetic regularities of the MnSi-electrode anodic dissolution were studied by the methods of polarization, capacitance, and impedance measurements. It was established that the addition of fluoride ions leads to weaker barrier properties of the silicon dioxide surface film, which determines the high silicide resistance in a fluoride-free medium. The order of the reaction was calculated for the MnSi anodic dissolution for NaF depending on the potential. In the region of low anodic potentials (from E_{cor} to $E \approx -0.2$ V), the reaction order ranged from 1.8 to 1.1, which was due to the high influence of silicon in the composition of the silicide and its oxidation products. With an increase in the polarization value (up to $E = 0.9$ V), the reaction order decreased to 0.5. An increase in the contribution of manganese ionization and oxidation reactions to the kinetics of the anodic dissolution of the silicide was observed. The silicide passivation in a fluoride-containing electrolyte was characterized by higher values of the dissolution current density (10^{-4}–10^{-3} A/cm^2) as compared to a fluoride-free electrolyte (10^{-6} A/cm^2), the reaction order in region of the passive state was ~1.0. Passivation was due to the formation of MnO_2 and SiO_2 oxides on the surface. In the transpassivation region ($E \geqslant 2.0$ V), there was a weak dependence of the current density on the concentration of fluoride ions. Oxygen release was observed on the surface of the electrode, and the formation of MnO_4^- ions was recorded in the near-electrode layer. The article discusses mechanisms and kinetic regularities of anodic processes on an MnSi-electrode in sulfuric acid solution in the presence of fluoride ions.

Keywords: Manganese monosilicide, Sulfuric acid electrolyte, Sodium fluoride, Anodic dissolution, Impedance

Для цитирования: Полковников И. С., Пантелеева В. В., Шеин А.Б. Анодное растворение и пассивация моносилицида марганца в сернокислых фторидсодержащих средах. *Конденсированные среды и межфазные границы*. 2024;26(2): 304–313. https://doi.org/10.17308/kcmf.2024.26/11941

For citation: Polkovnikov I. S., Panteleeva V. V., Shein A. B. Anodic dissolution and passivation of manganese monosilicide in fluoride-containing sulfuric acid solutions. *Condensed Matter and Interphases*. 2024;26(2): 304–313. https://doi.org/10.17308/kcmf.2024.26/11941

✉ Igor S. Polkovnikov, e-mail: igorpolkovnikov@mail.ru

1. Introduction

Many branches of science and technology face difficulties when using fluoride-containing solutions [1-10]. This mainly concerns enterprises involved in the production of metals from ores [3–6]. Due to the technological process, fluorides can accumulate in the water system and the fume-collecting chimney at the enterprise. The main danger of fluorides is associated with their concentration and the formation of hydrogen fluoride, which destroys metal structures and causes various types of corrosion [5, 6].

One way to protect steels from corrosion damage is to use alloying additives, which can affect the rate of steel dissolution in corrosive media. Metallurgy uses transition metal silicides as alloying additives, which are introduced into steel in the form of finished alloys or so-called ferroalloys (ferrosilicon, ferrosilicomanganese, ferromanganese, etc.). The introduction of ferrosilicomanganese into manganese silicide-based steel increases the wear and shock resistance of steel. It improves its corrosion characteristics due to the formation of surface barrier films and decreases the melting point of the alloy, which significantly reduces the cost of steel production [11–13]. A high content of silicon in steel favorably affects its elastic properties, resistance to corrosion and oxidation at high temperatures [11, 12, 14]. Manganese and iron form a solid solution, which increases steel hardness and strength. Manganese is used for desulfurization, which prevents the appearance of iron-sulfur bonds [13, 15].

The electrochemical behavior of manganese silicides (MnSi and Mn_5Si_3) in a fluoride-free acidic medium has been previously studied [16, 17]. These studies revealed high anode resistance of silicides due to the formation of a SiO_2-based barrier film on their surface. Since silicon dioxide is unstable in fluoride-containing media [18], it is expected that the anodic behavior of silicides will largely depend on the concentration of fluorides in the solution. This paper presents the results of the study of the anode resistance of manganese monosilicide MnSi in 0.5 M H_2SO_4 + (0.0025–0.05) M NaF solutions. This study revealed the concentration effect of sodium fluoride on the anodic dissolution and passivation of manganese monosilicide.

2. Experimental

Manganese monosilicide MnSi was obtained by the Czochralski method in the industrial single crystal growing furnace OKB-8093 ("Redmet-8"). The sample was pulled out using an alundum rod at a speed of 0.4 mm/min. To provide a better mixing of the melt and to create a more uniform temperature field, the crucible with melt and the seed were rotated in opposite directions with frequencies within the ranges of 0–15 and 0–60 rpm, respectively. The finished sample was placed in a fluoroplastic holder and filled with epoxy resin, which was then polymerized. The working area of the electrode surface was 0.1 cm^2.

Electrochemical measurements were carried out at a temperature of 25 °C under natural aeration conditions in unstirred 0.5 M H_2SO_4 + (0.0025–0.05) M NaF solutions. The solutions were prepared with chemically pure H_2SO_4, NaF reagents, and deionized water (water resistivity, 18.2 MΩ·cm, organic carbon content, 4 μg/l). Sodium fluoride was introduced into the solution immediately before the experiment.

Polarization and impedance measurements were taken using a Solartron 1255/1287 unit (Solartron Analytical) in an YASE-2 (pyrex glass) electrochemical cell with separated cathode and anode sections. A saturated silver chloride electrode was used as the reference electrode and a platinum electrode was used as the auxiliary electrode. The potentials in the work were given relative to the standard hydrogen electrode, the current densities i were given per unit of the geometric area of the electrode.

Cyclic current-voltage curves in a 0.5 M H_2SO_4 + 0.05 M NaF solution were recorded within the range from E corrosion to the anodic region at a potential sweep rate of ν = 10 mV/s. Before the measurement of the impedance spectra, the current was stabilized at each potential. After that, the impedance was measured at this value of E and higher potentials, and the potential was changed with a fixed step. Anodic potentiostatic curves for a given value of E were plotted based on the obtained i values. The range of frequencies $f(\omega/2\pi)$ used for impedance measurements was from 20 kHz to 0.02 Hz, while the amplitude of the alternating signal was 5–10 mV.

The morphology and surface composition of the samples before and after electrochemical

tests were investigated using a Hitachi S-3400N scanning electron microscope (Japan) with a Bruker Quantax 200 attachment for energy-dispersive analysis (Germany). The images were obtained in high vacuum at an acceleration voltage of 10 kV in the mode of secondary electron scattering.

The polarization and impedance data were measured and processed using the programs CorrWare2, ZPlot2, and ZView2 (Scribner Associates, Inc.).

3. Results and discussion

The anodic potentiostatic curves of the MnSi-electrode recorded in the potential range from E_{cor} to E = 3.2 B in solutions of H_2SO_4 with the addition of NaF are shown in Fig. 1. The introduction of fluoride ions into the solution resulted in significant changes in the shape of the silicide polarization curve. With an increase in the concentration of fluoride ions the anode peaks became noticeably more pronounced. The dissolution rate of MnSi in the 0.5 M H_2SO_4 solution containing a minimum concentration of NaF (at $E \approx 0.5$ V) was two orders of magnitude higher than that for a fluoride-free sulfuric acid solution. In the presence of fluoride ions, the transition to the transpassivation region occurred at higher anodic potentials.

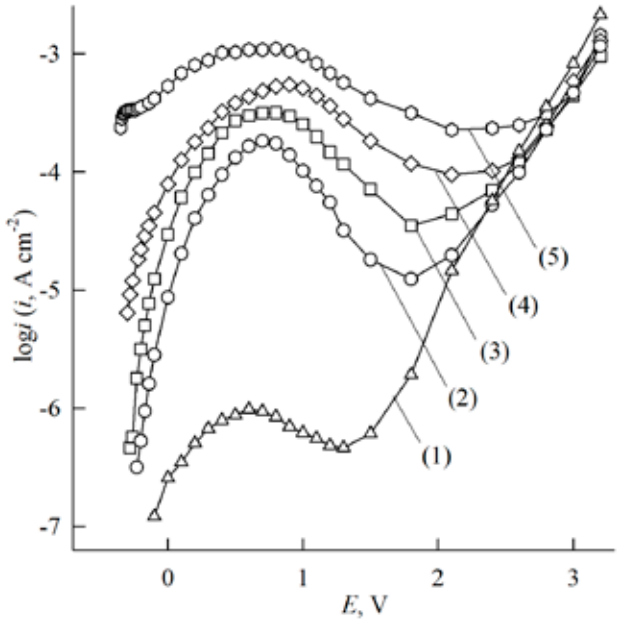

Fig. 1. Anodic potentiostatic curves of MnSi-electrode in 0.5 M H_2SO_4 (*1*) и 0.5 M H_2SO_4 + (*x*) M NaF, where *x* = 0.0025 (*2*); 0.005 (*3*); 0.01 (*4*), 0.05 (*5*)

Anodic polarization curves for manganese monosilicide in 0.5 M H_2SO_4 + (0.0025–0.05 M NaF) solutions can be divided into several characteristic sections. Section I (from E_{cor} to $E \approx -0.2$ V) corresponds to the region of active dissolution characterized by a rapid increase in current density with an increase in potential. In a solution with a concentration of 0.05 M NaF, a slight change in current was recorded. In this region, a weak gas emission was observed on the electrode surface. The intensity of gas formation decreased with an increase in the potential and a decrease in the concentration of NaF. According to [19], silicon in acidic media is oxidized to form silicon dioxide, which can dissolve in the presence of HF. According to [20, 21], during the oxidation of silicon in fluoride-containing media in the region of low anodic polarizations hydrogen can form on its surface. Manganese in acidic media is unstable, it can spontaneously dissolve with the release of hydrogen [22, 23]. Along with chemical dissolution, there is electrochemical oxidation of manganese with the formation of Mn^{2+} ions. The transformations of silicon and manganese in this section of the polarization curve can be described by the following equations:

$$Si + 2H_2O = SiO_2 + 4H^+ + 4e^-, E^0 = 0.86 \text{ V}; \quad (1)$$

$$SiO_2 + 6HF = H_2SiF_6 + 2H_2O; \quad (2)$$

$$Mn + H_2SO_4 = MnSO_4 + H_2; \quad (3)$$

$$Mn = Mn^{2+} + 2e^-, E^0 = -1.18 \text{ V}. \quad (4)$$

On the surface of MnSi in a 0.5 H_2SO_4 solution without the addition of NaF at low anodic potentials there was no gas release. Manganese in the composition of the silicide in a fluoride-free electrolyte was more stable due to the formation of a silicon dioxide surface film [16, 17]. The addition of sodium fluoride weakened the passivation action of silicon dioxide and thus led to the activation of the processes of manganese and silicon dissolution in the composition of the silicide, which, apparently, was accompanied by the release of hydrogen.

Section II (from –0.2 V to 0.9 V) is characterized by a further increase in the density of the silicide dissolution current, however, the rate of i increase fell with an increase in E (the slope of the polarization curve changed). With an increase in the concentration of NaF, the range

of the recorded anode peak markedly expanded. Section III (from 0.9 V to 2.0 V) is characterized by a gradual decrease in current density which ends with a narrow passivation region. Section IV (from 2.0 to 3.2 V) characterizes the passivation region. At this section of the polarization curves at $E > 2.6$ V small gas (oxygen) bubbles formed on the surface of the electrode and the space near the electrode was colored crimson. As compared to the fluoride-free solution, oxygen release was observed at higher values of potential (in a fluoride-free medium at $E \geqslant 2.2$ V).

The kinks on the MnSi-electrode polarization curves in the fluoride-containing electrolyte are probably related to the formation of manganese oxides:

$$Mn + H_2O = MnO + 2H^+ + 2e^-, E^0 = -0.65 \text{ V}; \quad (5)$$

$$Mn + 3H_2O = Mn_2O_3 + 6H^+ + 6e^-, E^0 = -0.31 \text{ V}; \quad (6)$$

$$Mn_2O_3 + H_2O = 2MnO_2 + 2H^+ + 2e^-, E^0 = 1.0 \text{ V}; \quad (7)$$

$$Mn^{2+} + 2H_2O = MnO_2 + 4H^+ + 2e^-, E^0 = 1.23 \text{ V}. \quad (8)$$

The solubility of manganese (II) oxide in acidic media is quite high, and it cannot cause deep passivation of the electrode [24]. According to [22], the passivation of manganese is possibly due to the formation of Mn_2O_3 and MnO_2 oxides on its surface. However, manganese (III) oxide in an acidic medium is unstable and disproportionate to the formation of manganese (II) and (IV) compounds. Manganese dioxide is more stable in acids and its formation can cause passivation of the electrode. Oxidation of manganese dioxide with the formation of permanganate ions leads to its removal from the surface of the electrode [23]:

$$MnO_2 + 2H_2O = MnO_4^- + 4H^+ + 2e^-, E^0 = 1.69 \text{ V}. \quad (9)$$

The results of microscopic examination of the surface of manganese monosilicide before and after electrochemical tests are shown in Fig. 2. Anodic polarization of the MnSi-electrode in a 0.5 M H_2SO_4 solution caused partial etching of the electrode surface (Fig. 2b). The addition of fluoride ions to the solution (Fig. 2c) led to the formation of a more developed surface relief, there were pronounced convex regions.

Elemental analysis of the silicide surface (Table 1) showed that in the fluoride-free solution the surface layer of the electrode was depleted of manganese and there was an increase in the oxygen content (as compared to the original sample). The latter was probably due to the selective dissolution of manganese from the silicide surface layer at low anodic polarizations and due to the oxidation of silicon to low-soluble silicon in the acidic media of silicon dioxide. In

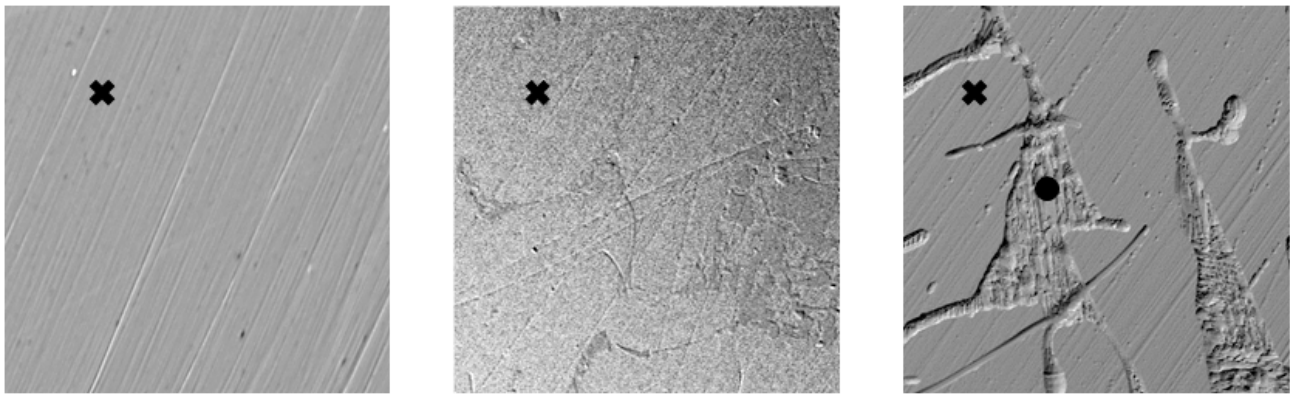

a b c

Fig. 2. Microphotographs of MnSi surface (×400) before (a) and after etching in 0.5 M H_2SO_4 (b) and 0.5 M H_2SO_4 + 0.05 M NaF (c) at $E = 3.2$ V

Table 1. Elemental analysis of the MnSi electrode surface at the point (Fig. 2)

Elements		Mn, at.%	Si, at.%	O, at.%
Initial sample		46.5±2.3	49.6±2.5	3.9±0.2
Sample after polarization from E_{cor} to $E = 3.2$ V at $\nu = 0.1$ mV/s	in 0.5 M H_2SO_4	21.2±0.6	58.4±2.9	20.6±0.6
	in 0.5 M H_2SO_4 + 0.05 M NaF (×)	45.9±2.3	49.3±2.5	4.8±0.2
	in 0.5 M H_2SO_4 + 0.05 M NaF (●)	28.5±1.4	31.3±1.6	40.2±2.0

the fluoride-containing electrolyte, an increased oxygen content was recorded in the region of the convex areas; the ratio of the amount of manganese and silicon corresponded to the ratio of the elements in the MnO_2 and SiO_2 oxides. Outside the convex region, the composition of the silicide surface differed slightly from that of the original sample.

Similar dependencies indicate the formation of oxides on the MnSi surface with its anodic polarization up to 3.2 V. In a fluorine-free medium, a film consisting mainly of silicon dioxide was formed; in the presence of sodium fluoride, manganese and silicon oxides (probably MnO_2 and SiO_2) were formed, which partially dissolved in the solution when interacting with the components of the electrolyte.

The degree of fluoride ion concentration influencing the rate of anodic processes on the silicide is shown in Fig. 3. It can be seen that the dependence of the reaction order $n_{NaF}=\partial \lg i/\partial \lg C_{NaF}$ of the manganese monosilicide anodic dissolution for F^- ions is a mirror reflection of the anodic curve with the lowest of the studied sodium fluoride concentrations equal to 0.0025 M. At low concentrations of fluoride

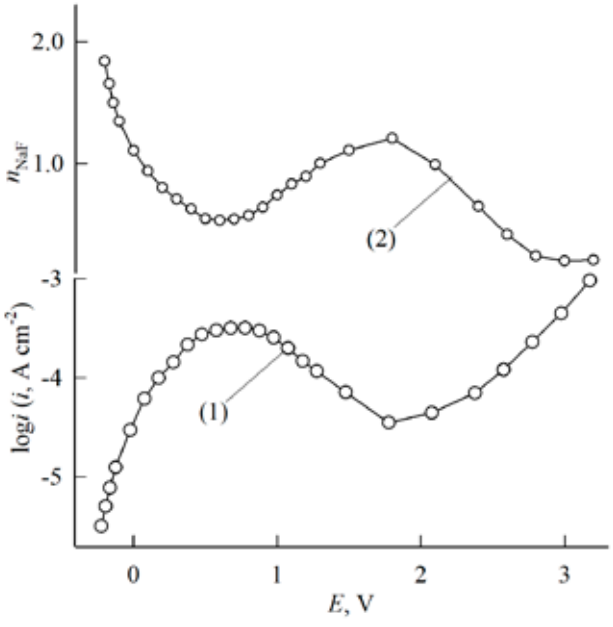

Fig. 3. Graphs of the dependences of electrochemical quantities on the potential of the MnSi-electrode: (*1*) Anodic potentiostatic curve in 0.5 M H_2SO_4 + 0.0025 M NaF; (*2*) The dependence of n_{NaF} on the potential in 0.5 M H_2SO_4 + (0.0025–0.05) M NaF

ions, the content of silicon dioxide on the silicide surface was still high and the rate of the oxidation process seemed to be limited by the rate of dissolution of silicon dioxide interacting with HF (which formed when NaF was introduced into an acidic medium). The film thickness at each potential value was determined by the successive processes of electrochemical oxidation of silicon and chemical dissolution of silicon dioxide until it reached a steady state.

Previous research [18] distinguishes two ways of dissolving silicon dioxide depending on the amount of silicon in the samples. With a high silicon content in silicides, silicon atoms are not isolated from each other, which can lead to the formation of ≡Si-O-Si≡ siloxane groups, therefore, etching will proceed according to equation (10) and a second reaction order for HF should be expected:

$$\equiv Si\text{-}O\text{-}Si\equiv + 2HF \rightarrow 2 \equiv Si\text{-}F + H_2O. \quad (10)$$

With a low silicon content, isolated Si-OH silanol groups can be formed, the limiting stage of their dissolution will be reaction 11, according to which the HF reaction order is equal to one:

$$\equiv Si\text{-}OH + HF \rightarrow \equiv Si\text{-}F + H_2O. \quad (11)$$

As a result of the silicon dioxide dissolution, the processes associated with the ionization of manganese are activated. The electrochemical dissolution of manganese in acidic media can be represented by the following stages [25]:

$$Mn + H_2O = MnOH_{ads} + H^+ + e^-; \quad (12)$$

$$MnOH_{ads} + H^+ = Mn^{2+} + H_2O + e^-. \quad (13)$$

When the solution contains hydrofluoric acid, HF molecules can take part in the process of manganese ionization, for example, according to the scheme:

$$Mn + HF = MnF_{ads} + H^+ + e^-; \quad (14)$$

$$MnF_{ads} + H^+ = Mn^{2+} + HF + e^-. \quad (15)$$

Due to the fact that the dissolution of silicon dioxide is characterized by the first (reaction 11) or second (reaction 10) order for HF and the dissolution of manganese has the first order (reaction 14), it can be concluded that in the region of the first anodic section the process of the MnSi-electrode dissolution will be predominantly determined by the dissolution of silicon dioxide.

The values for the reaction order in this region gradually decreased from 1.8 to 1.1 (Fig. 3), which seems to indicate the mixed nature of the bonds on the silicide surface: both silanol and siloxane groups were present.

With increasing polarization, the values of the reaction order decreased to ~ 0.5; according to Fig. 3, the minimum of the reaction order corresponded to the maximum on the anodic curves ($E \approx 1.0$ V). The papers [22-24, 26] describe the abnormal dissolution of manganese in acidic fluoride-free media, while in the silicide composition manganese is more stable [16, 17]. The addition of sodium fluoride appears to activate the anodic dissolution of manganese from the silicide. As a result, the recorded current mainly corresponded to the processes of manganese oxidation and dissolution (reactions 3, 4, and 5), which were weakly dependent on the presence of HF in the composition of the electrolyte. The latter caused low n_{NaF} values.

At $E > 0.9$ V, the reaction order began to gradually increase and reached a peak at the potentials of the passivation region on the polarization curves. Apparently, this was due to the accumulation of passivating products of manganese and silicon anodic oxidation (Mn_2O_3, MnO_2, and SiO_2 oxides) on the surface of the electrode, which dissolved with the participation of HF molecules. The authors of [27, 28] proposed a scheme for the process of nickel (II) and iron (III) oxides dissolution in an acidic fluoride-containing electrolyte. According to [28], for manganese (IV) oxide it is:

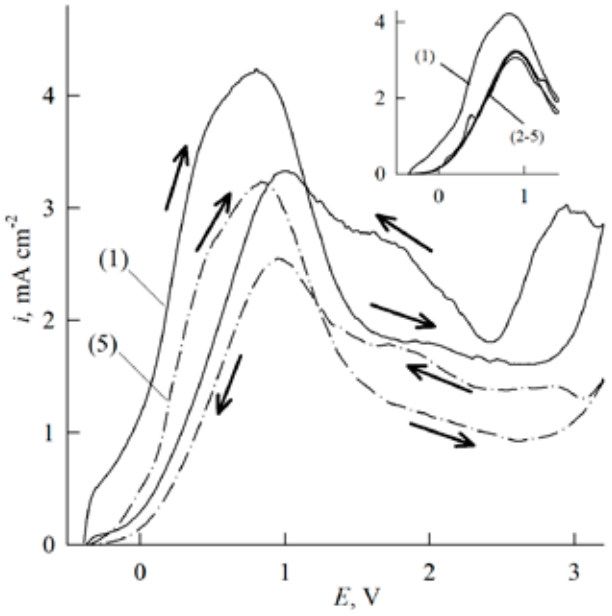

Fig. 4. Cyclic voltammetric curves of the MnSi-electrode in 0.5 M H_2SO_4 + 0.05 M NaF. The number is the polarization cycle. In the upper right corner - 5 cycles of polarization at the reversal potential E_{revers} = 1.4 V

$$Mn_{ox}^{4+} + HF = MnF_{ads}^{3+} + H^+; \quad (16)$$

$$MnF_{ads}^{3+} + 5HF = [MnF_6]^{2-} + 5H^+. \quad (17)$$

In the transpassivation region, the reaction order approaches zero.

The shape of CVA curves indicates the occurrence of several MnSi-electrode oxidation and dissolution processes in a fluoride-containing electrolyte (Fig. 4). In the first polarization cycle, three anode peaks in both forward and reverse directions were recorded on the CVA curve in the potential range from E_{cor} to E = 3.2 V. As the number of the polarization cycle increased, a slight decrease in the values of the dissolution current density were observed. With a gradual decrease in the reversal potential, first to 2.2 V (up to the passivation region), then to 1.4 V (up to the beginning of the passivation region), the shape of the CVA curves in the forward and reverse directions remained unchanged. A more noticeable decrease in the manganese silicide dissolution currents with an increase in the polarization cycle at a reversal potential of 3.2 V as compared to E reversal to 1.4 and 2.2 V indicates the accumulation of passivating products of anodic oxidation on the silicide surface which were not completely removed in the presence of fluoride and caused partial passivation of the electrode.

Fig. 5 shows the dependence of the differential capacitance of the MnSi-electrode on the potential in semi-logarithmic coordinates. The values of the differential capacitance were calculated from the ratio $C = -1/(\omega Z'')$, where ω is the angular frequency of the alternating current, Z'' is the imaginary part of impedance at a frequency of 10 kHz. The maximum values of the differential capacitance were observed at potentials close to E_{cor} and were ~16.5 μF/cm² in a solution containing 0.05 M NaF. With a gradual increase in the potential, the differential capacity decreased sharply. The drop was sharper with a higher concentration of fluoride ions in the solution. At potentials above 1.0 V, the values of

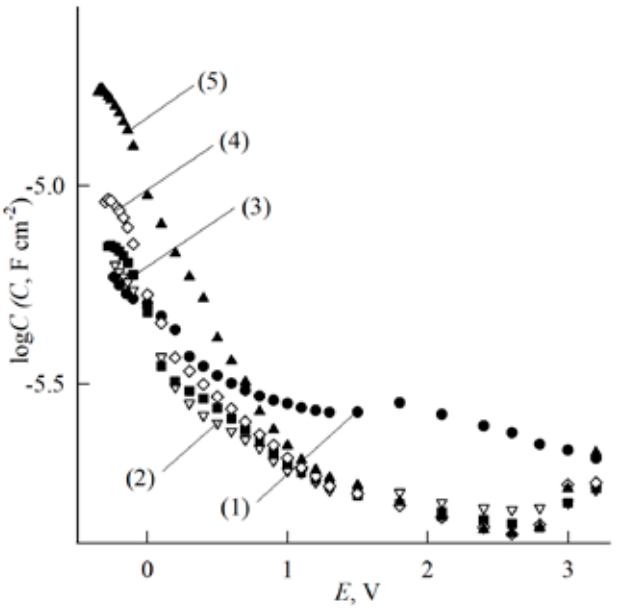

Fig. 5. Dependence of the logarithm of the differential capacitance on the potential of the MnSi-electrode in 0.5 M H_2SO_4 (*1*) and 0.5 M H_2SO_4 + (*x*) M NaF, where *x* = 0.0025 (*2*); 0.005 (*3*); 0.01 (*4*), 0.05 (*5*)

the differential capacitance did not depend on the concentration of fluoride ions. Similar to the polarization curves (Fig. 1), *C*,*E* -dependencies can be divided into four linear sections, the change in the slope of which indicates changes in the surface state. A gradual decrease in the values of the differential capacitance from 16.5 to 2 μF/cm² may indicate the formation of compounds on the silicide surface characterized by low conductivity (resistivity $\rho(SiO_2) \approx (10^{12}–10^{16})$ Ω·cm [21]; $\rho(Mn_2O_3) \approx 10^5$ Ω·cm; $\rho(MnO_2) \approx (10^{-1}–10^{2})$ Ω·cm [29]). According to reactions 10 and 11, a large number of Si-F bonds should be expected. According to authors [30, 31], the polarizability of Si-F bonds is less than that of Si-OH bonds.

The MnSi-electrode impedance spectra in sulfuric acid solutions with the addition of sodium fluoride are more complex than in a fluoride-free solution [16]. The form of the impedance spectra changed with the shape of the polarization curve and the variation in the concentration of fluoride ions (Fig. 6), which indicates the diversity of the silicide dissolution and passivation processes.

At the potentials of anodic section I, in solutions with a low concentration of NaF (⩽ 0.01 M), capacitive semicircles with the center in the region *Z″* > 0 were recorded on the complex

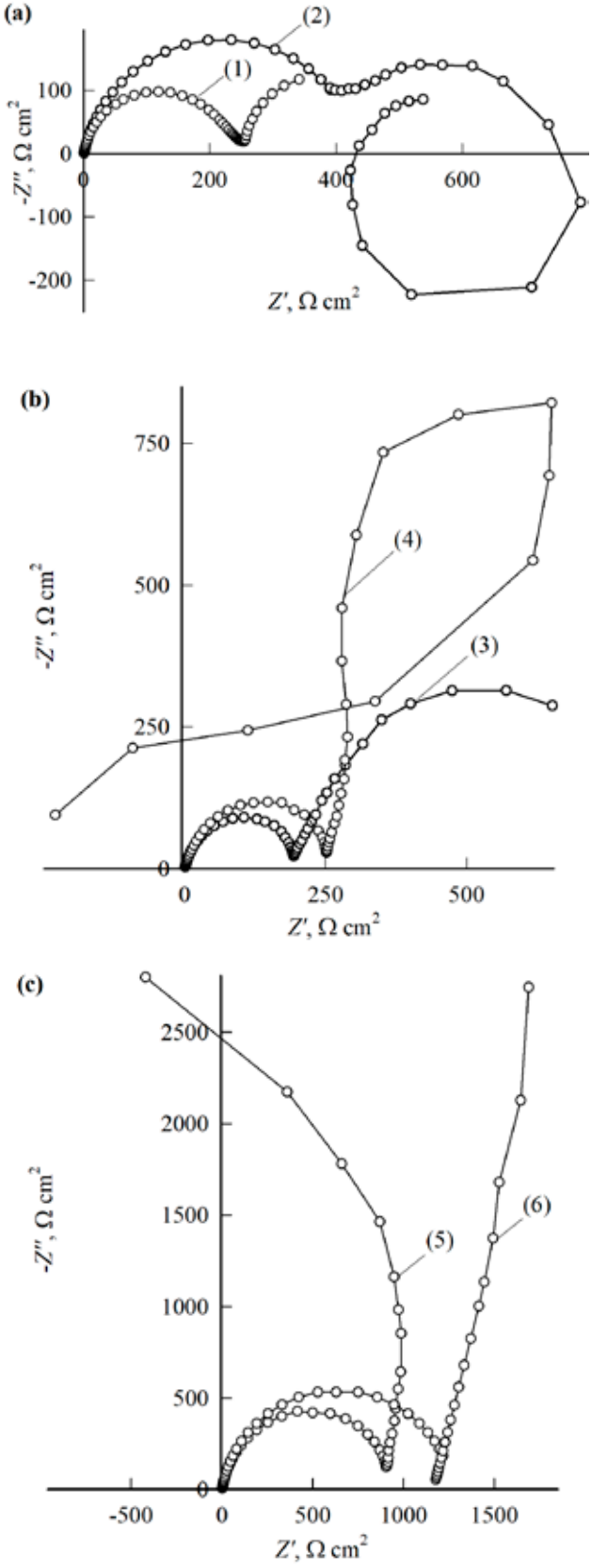

Fig. 6. Impedance spectra of MnSi electrode in 0.5 M H_2SO_4 + 0.05 M NaF at *E*, V: -0.32 (*1*); 0 (*2*); 0.9 (*3*); 1.1 (*4*); 1.8 (*5*); 2.6 (*6*)

Z-plane. The system was characterized by high values of the impedance modulus $|Z|$ (~90 kΩ·cm^2). $|Z|$ increased with an increase in polarization. Similar dependencies were also observed for MnSi in a fluoride-free sulfuric acid solution ($|Z| \approx 250$ kΩ·cm^2), in which the behavior of the silicide was determined by a silicon dioxide barrier film [16]. Apparently, with a low content of fluoride ions, the passivating effect of silicon dioxide persists, but the barrier properties of the oxide film weaken. With a concentration of NaF equal to 0.05 M, an additional capacitive semicircle appeared on the impedance spectra in the low frequency (LF) region (Fig. 6A). This indicates the staged nature of the oxidation processes of the components of manganese silicide, which are accompanied by adsorption of intermediates on the electrode surface (reactions 10–15). The form of the impedance spectra confirms the assumptions made on the basis of constant current measurements and calculations of the n_{NaF} reaction order.

The impedance spectra in the potential region of anodic section II (Fig. 6a, E = 0 B) contained several semicircles: at least two capacitive semicircles in the high-frequency (HF) region, one inductive semicircle, and one capacitive arc in the low-frequency region. With an increase in the potential, the diameter of the low-frequency semicircles decreased and at certain potentials several loops were recorded. More complex impedance graphs as compared to the graphs in section I indicates the presence on the silicide surface in this region of the potentials of several types of intermediates formed during the manganese and silicon ionization (reactions 10–12, 14). Intermediates formed during the dissolution of manganese (II) oxide in the presence of fluoride ions were probably also recorded.

When the anodic polarization curve approached its maximum (at E from 0.5 to 0.8 V), an increase in the diameter of the second capacitive semicircle was observed. Near the maximum $E \approx 0.9$ V, this section of the impedance spectra had the form of an almost vertical straight line, in the low-frequency region a distorted capacitive semicircle was also recorded (Fig. 6b). At the end of anodic section III (at E = 1.8 V), the impedance spectra contained a high-frequency capacitive semicircle and a low-frequency semicircle, which at $\omega \to 0$ was recorded in the region of negative Z'. With a further increase in potential, the diameter of the LF semicircle increased markedly faster than the diameter of the HF semicircle (Fig. 6c). The form of impedance spectra indicates the occurrence of passivation processes (reactions 1, 5–8), which correlated with the region of negative slope di/dE on the anodic polarization curves at these E (Fig. 1).

In the region of oxygen release potentials, the impedance spectra of manganese silicide in a fluoride-containing electrolyte had the same form as in a fluoride-free solution, i.e. two well-divided capacitive semicircles. At maximum polarization (E = 3.2 V), an inductive low-frequency arc was also observed. The latter indicates the destruction of the oxide film on the surface of the MnSi-electrode in a fluoride-free solution and the removal of manganese and silicon oxides (MnO_2 and SiO_2) in the fluoride-containing electrolyte, which provides for a release of oxygen.

4. Conclusions

The study of the anodic behavior of the MnSi-electrode in 0.5 M H_2SO_4 + (0.0025 – 0.05) M NaF solutions indicates a strong influence of fluoride ions on the processes of anodic dissolution and passivation of silicide. The silicon dioxide surface film, which is stable in acid, dissolves when fluoride ions are added. As a result, the process of anodic dissolution of manganese monosilicide is activated. It was established that at low anodic polarizations (from E_{cor} to $E \approx -0.2$ V), the influence of silicon dioxide persists, the rate of its dissolution determines the anode resistance of the silicide. In the potential range (from –0.2 V to 0.9 V), manganese ionization and oxidation reactions (up to Mn^{2+}, MnO) make a significant contribution to the kinetics of anodic processes. Manganese monosilicide passivation is observed at potentials (from 0.9 V to 2.0 V) and is associated with the formation of manganese and silicon oxides (Mn_2O_3, MnO_2, and SiO_2). In the region of transpassivation (from 2.0 to 3.2 V), the processes of oxygen release and further manganese oxidation (up to MnO_4^-) are recorded.

Contribution of the authors

The authors contributed equally to this article.

Conflict of interests

The authors declare that they have no known competing financial interests or personal relationships that could have influenced the work reported in this paper.

References

1. Aoun A., Darwiche F., Hayek S. A., Doumit J. The fluoride debate: the pros and cons of fluoridation. *Preventive Nutrition and Food Science*. 2018;23(3): 171–180. https://doi.org/10.3746/pnf.2018.23.3.171

2. Genuino H. C., Opembe N. N., Njagi E. C., McClain S., Suib S. L. A review of hydrofluoric acid and its use in the car wash industry. *Journal of Industrial and Engineering Chemistry*. 2012; 18(5): 1529–1539. https://doi.org/10.1016/j.jiec.2012.03.001

3. Bordzilowski J., Darowicki K. Anti-corrosion protection of chimneys and flue gas ducts. *Anti-Corrosion Methods and Materials*. 1998;45(6): 388–396. https://doi.org/10.1108/00035599810236243

4. Palazzo A. Fluoride corrosivity on mild steel in cooling systems. *Materials Performance*. 2017;56: 44–48. Available at: https://www.materialsperformance.com/articles/material-selection-design/2017/07/fluoride-corrosivity-on-mild-steel-in-cooling-systems

5. D'yachenko A. N., Kraydenko R. I., Kurchenko E. I. Corrosion resistance of steels and alloys in fluoride salts. *Bulletin of PNRPU. Mechanical Engineering, Materials Science*. 2017;19(4): 75–89. (In Russ., abstract in Eng.). https://doi.org/10.15593/2224-9877/2017.4.05

6. Dai H., Shi S., Yang L., Guo C., Chen X. Recent progress on the corrosion behavior of metallic materials in HF solution. *Corrosion Reviews*. 2021;39(4): 313–337. https://doi.org/10.1515/corrrev-2020-0101

7. Luo Z., Zuo J., Jiang H., ... Wei W. Inhibition effect of fluoride ion on corrosion of 304 stainless steel in occluded cell corrosion stage in the presence of chloride ion. *Metals*. 2021;11(350): 1–16. https://doi.org/10.3390/met11020350

8. Guo S., Zhang J., Wu W., Zhou W. Corrosion in the molten fluoride and chloride salts and materials development for nuclear applications. *Progress in Materials Science*. 2018;97: 448–487. https://doi.org/10.1016/j.pmatsci.2018.05.003

9. Nikitina E. V., Karfidov E.A., Zaikov Yu. P. Corrosion of advanced metal materials in fluoride meltsfor liquid salt reactors. *Melts*. 2021;1: 21–45. (In Russ., abstract in Eng.). https://doi.org/10.31857/S0235010621010072

10. Kerroum Y., Guenbour A., Bellaouchou A., Idrissi H., García-Antón J., Zarrouk A. Chemical and physical effects of fluoride on the corrosion of austenitic stainless steel in polluted phosphoric acid. *Journal of Bio- and Tribo-Corrosion*. 2019;5(3): 68. https://doi.org/10.1007/s40735-019-0261-5

11. Ulyanin E. A., Svistunova T. V., Levin F. L. *Highly alloyed corrosion-resistant alloys**. Moscow: Metallurgiya Publ.; 1987. 88 p. (in Russ.).

12. Tolmanov N. D., Chernova G. P. *Corrosion and corrosion-resistant alloys**. Moscow: Metallurgiya Publ.; 1973. 231 p. (In Russ).

13. Mysik V. F., Zhdanov A. V., Pavlov V. A. *Metallurgy of ferroalloys: technological calculations: a textbook**. Ekaterinburg: Ural University Publishing House; 2018. 536 p. (In Russ). Available at: https://elar.urfu.ru/handle/10995/64931

14. Maznichevsky A. N., Goikhenberg Yu. N., Sprikut R. V. Influence of silicon and microalloying elements on the corrosion resistance of austenitic steel. *Bulletin of the South Ural State University. Series "Metallurgy"*. 2019;19(2): 14–24. (In Russ., abstract in Eng.). https://doi.org/10.14529/met190202

15. Handayani D., Okhuysen V., Wagner N. Machinability of high Mn steel using tool life criteria. *International Journal of Metalcasting*. 2023;17(3): 1–8. https://doi.org/10.1007/s40962-023-01044-3

16. Russkikh M. A., Polkovnikov I. S., Panteleeva V. V., Shein A. B. Passivation on manganese monosilicide in sulfuric acid electrolytes. *Bulletin of Perm University. Chemistry*. 2020;10(2): 50–59. (In Russ., abstract in Eng.). https://doi.org/10.17072/2223-1838-2020-2-221-232

17. Polkovnikov I. S., Panteleeva V. V., Shein A. B. Anodic dissolution and passivation of Mn_5Si_3 electrode in acidic and alkaline media. *Bulletin of Perm University. Chemistry*. 2019;9(3): 250–265. (In Russ., abstract in Eng.). https://doi.org/10.17072/2223-1838-2019-3-250-265

18. Knotter D. M. Etching mechanism of vitreous silicon dioxide in HF-based solutions. *Journal of the American Chemical Society*. 2000;122(18): 4345–4351. https://doi.org/10.1021/ja993803z

19. Lehmann V. *Electrochemistry of silicon: instrumentation, science. Materials and applications*. Weinheim: Wiley–VCH Verlag GmbH; 2002. 273 p. https://doi.org/10.1002/3527600272

20. Memming R., Schwandt G. Anodic dissolution of silicon in hydrofluoric acid solutions. *Surface Science*. 1966;4: 109–124. https://doi.org/10.1016/0039-6028(66)90071-9

21. Zhang X. G. *Electrochemistry of silicon and its oxide*. New York: Kluwer Academic/ Plenum Publ.; 2001. 510 p.

22. Agladze R. I., *Manganese electrochemistry**. Tbilisi: Publishing House of the Academy of Sciences of the GSSR; 1957. 518 p. (In Russ).

23. Kemmitt R. D. W., Peacock R. D. *The chemistry of manganese, technetium and rhenium*. Pergamon;

1973. 876 p. https://doi.org/10.1016/B978-0-08-018870-6.50005-6

24. Kolotyrkin Y. M., Agladze T. R. Chemical dissolution of manganese*. *Protection of Metals*. 1968;4(6): 721–724. (In Russ).

25. Burstein G. T., Wright G. A., The anodic dissolution of nickel. I. Perchlorate and fluoride electrolytes. *Electrochimica Acta*. 1975;20: 95–99. https://doi.org/10.1016/0013-4686(75)85049-3

26. Toro N., Saldaña M., Gálvez E., ... Hernández P. C. Optimization of parameters for the dissolution of Mn from manganese nodules with the use of tailings in an acid medium. *Minerals*. 2019;9(7): 387–398.https://doi.org/10.3390/min9070387

27. Löchel B., Strehblow H.-H., Sakashita M. Breakdown of passivity of nickel by fluoride. *Journal of The Electrochemical Society*. 1984;131(3): 522–529. https://doi.org/10.1149/1.2115620

28. Löchel B., Strehblow H.-H. Breakdown of passivity of iron by fluoride. *Electrochimica Acta*. 1983;28(4): 565–571. https://doi.org/10.1016/0013-4686(83)85043-9

29. Lazarev V. B., Krasov V. G., Shaplygin I. S. *Electrical conductivity of oxide systems and film structures**. Moscow: Nauka Publ.; 1978. 168 p. (In Russ).

30. Baklanov M. Green M., Maex K. *Dielectric films for advanced microelectronics*. John Wiley & Sons; 2007. 512 p. https://doi.org/10.1002/9780470017944

31. Seshan K., Schepis D. *Handbook of thin film deposition*. Norwich, New York, U.S.A.: William Andrew Publ.; 2018. 470 p. https://doi.org/10.1016/b978-0-12-812311-9.00030-x

**Translated by author of the article*

Information about the authors

Igor S. Polkovnikov, Postgraduate student at the Department of Physical Chemistry, Perm State University (Perm, Russian Federation).
https://orcid.org/0000-0003-4381-6467
igorpokovnikov@mail.ru

Viktoria V. Panteleeva, Cand. Sci. (Chem.), Associate Professor, Department of Physical Chemistry, Perm State University (Perm, Russian Federation).
https://orcid.org/0000-0002-1506-6665
vikpant@mail.ru

Anatoliy B. Shein, Dr. Sci. (Chem.), Professor at the Department of Physical Chemistry (Perm State University (Perm, Russian Federation).
https://orcid.org/0000-0002-2102-0436
ashein@psu.ru

Received 06.06.2023; approved after reviewing 24.11.2023; accepted for publication 15.12.2023; published online 25.06.2024.

Translated by Irina Charychanskaya